Hydrodynamic study of the Single-Stirred Membrane Filtration Module: A CFD-based approach

[1]Keka Rana and [2]Debasish Sarkar*

[1]Department of Chemical Engineering, Haldia Institute of Technology, Haldia, PurbaMedinipur, West Bengal, India

[2]Department of Chemical Engineering, University of Calcutta, Kolkata 700 009, West Bengal, India

ABSTRACT

Membrane based separation technologies are nowadays very often recommended over the traditional separation techniques because of their simple modular design, low power consumption, easy way handling, and hazard-free operation. A large number of membrane modules were proposed over time to suit for the specific operational requirement. For instance, the Dynamic Shear Enhanced membrane filtration units, which include Rotating Disk, Rotating Disk-Membrane, Vibratory Shear Enhanced Processing units, Multi-Shaft Disk, and many others, were introduced to generate feed flow independent high shear rate at the membrane surface to effectively alleviate the problems of concentration polarization and membrane fouling. The single-stirred cell, alternatively known as rotating disk device, is recognized as one of the baseline DSE modules. The design is pretty simple. The module is a dead-end unit with a flat disk stirrer placed close to the membrane surface. Imperatively, many experimental studies have been reported on the performance of the Dynamic Shear Enhanced filtration devices. Nevertheless, reports on the corresponding hydrodynamic analysis are quite rare. The present work demonstrates the fundamental hydrodynamic characteristics, such as the velocity field and the shear stress distribution, of a single-stirred cell using CFD. The k-ε realizable turbulent model was chosen to simulate this module. Analysis was based on the variation of transmembrane pressure and rotational velocity.

Keywords: Computational fluid dynamics, Concentration polarization, Fouling, Membrane separation, Single-stirred cell

1. Introduction

Membrane based process is now-a-days widely recognized as a promising separation technology. The simple design, low energy consumption, efficient separation, and easy handling of membrane-based processes relatively favors their applications in pharmaceutical, food and biochemical industries over the conventional separation techniques [1].In spite of the advantages, expected growth of membrane technology is hindered owing to the two nonidealities, namely reversible concentration polarization and irreversible fouling [2-4], which is majorly stimulated by the polarization effect.

A large volume of works on the concentration polarization (CP), were reported, which were primarily based on the origin, development, influence of other physical parameters (e.g., viscosity, feed concentration, transmembrane pressure etc.), thermodynamic interpretation, and its relation with the membrane fouling [2, 5-7].Similarly, an abundance of curative works is recorded to mitigate fouling [8-12]. It has been established that the fouling is controlled efficiently by limiting the degree of CP. Furthermore, researchers have also demonstrated the efficacy of high shear generation near the membrane surface to efficiently control the CP and the subsequent fouling [13-14].

The cross-flow modules were first introduced in late 1960s [15] with the primary intention to limit the growth of polarized layer, which was accomplished by high shear generation at the membrane surface. However, the shear generation is entirely dependent on the feed velocity. High velocity helps to increase the velocity gradient close to the membrane surface. At the same time, it increases the pumping cost and also leads to a non-optimal distribution of the transmembrane pressure from the feed inlet to the retentate outlet. As a consequence permeate throughput decreases along the axial length of the device [16]. To overcome this problem in an ultrafiltration cell, the design has been again shifted to the dead-end type, and a stirrer is placed in a close proximity of membrane to generate a high shear over there. This module is popularly known as "single stirred cell". Following the same design principle, Rotating Disk-Membrane (RDM) and Multi-Shaft Disk (MSD) were introduced later [17]. In the RDM module, the membrane and the stirrer rotates in opposite direction with respect to each other. The counter-rotating membrane-stirrer assembly is expected to produce a more intense shear field compared to the single-stirrer cell. Consequently, a RDM module may be recognized as an updated design of the baseline single-stirred cell. The MSD is further upgraded not only in terms of shear generation, but also from the perspective of high membrane packing area per unit volume of the module [16, 18]. The three filtration devices (i.e., single-stirred, RDM, and MSD) were extensively characterized in treatment of different feed solutions and suspensions including Kraft black liquor, PEG-6000 solution, desizing wastewater, BSA solution, whey proteins, and mineral suspensions [14, 16, 19 - 20]. At the same time, literature review also indicates relatively fewer number of modeling and simulation studies. Some of the models based on the concept of back transport flux, surface renewal theory, and film theory have been proposed and validated [14, 21 - 23].Closer investigation reveals that the lack of the simulation studies is principally caused by the complex hydrodynamic environment inside the module, which complicates the whole modelling exercise. Thus, it is quite evident that primarily to begin, we must have a thorough knowledge of the hydrodynamic environment that prevails in the specific DSE module of interest. Considering the simplicity of the design, one may begin with the single-stirred cell.

The current study presents a hydrodynamic characterization study of a single-stirred membrane filtration cell using the well-known Computational fluid dynamics (CFD) approach. Different hydrodynamic variables, such as the velocity field, shear stress, turbulent kinetic energy, and kinetic energy dissipation rates within default interior of the unit have been simulated under varying parametric conditions (i.e., transmembrane pressure and rotational speed of the basket). The results clearly justify the changing performance of the device under different parametric states that lies within the scope of the present study.

2. Materials and methods

2.1. Single-stirred cell

The basic design is very similar to the cylindrical dead-end module in which the membrane is placed at the base of the cylinder. However, in the single-stirred module we have an additional flat-disk stirrer mounted on an overhung shaft. The disk and the membrane have the same diameter. The disk is placed face to face with the membrane having a very small gap. This small clearance facilitates a high shear generation at the membrane surface. Thus, the CP is expected to be alleviated. The schematic of the single-stirred cell is shown in Fig. 1.

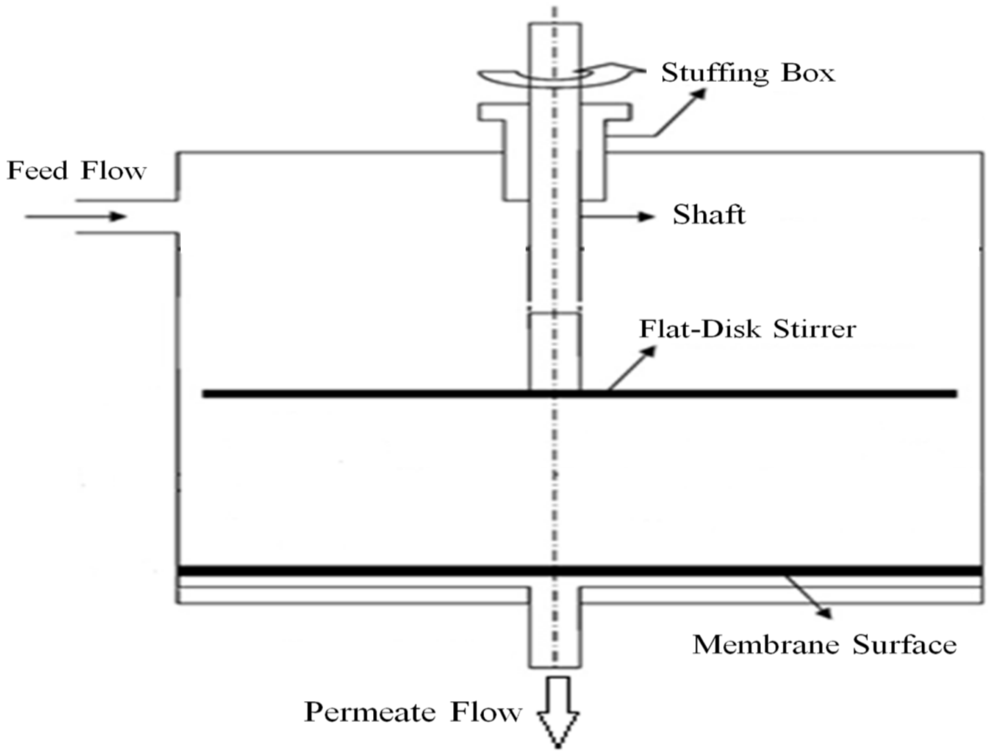

Fig. 1: Schematic of the single-stirred ultrafiltration cell

3. CFD Simulation and Model Analysis

3.1. Model assumptions

Standard hydrodynamic simulation was carried out for the single-stirred module considering relatively negligible permeate flow compared to the retentate flow rate. The governing continuity and momentum equations were solved using the finite volume method (FVM) in GAMBIT and FLUENT platform. The disk rotates within the module facing no other obstruction. Therefore, rotating reference frame was selected for the present simulation scheme.

The model assumptions are listed as under

i) Steady and incompressible flow of Newtonian fluid
ii) No-slip at solid boundaries.
iii) Pressure Inlet Boundary condition was used as the inlet and the outlet pressures are directly obtained from the respective pressure gauge readings.
iv) Flow regime is turbulent.

3.2. Grid generation

GAMBIT (2.3.16) was used to mesh the flow domain. Finer grid always gives better accuracy at the cost of higher computation time. Hence, optimization of grid should be necessarily performed in any CFD analysis. Generally, finer grid is generated at larger gradient zone, whereas courser grid is selected for uniform flow regime. Presently, we have performed the grid independence test for to ensure optimal grid generation.

3.3 Modeling and solution

FLUENT (6.3.26) was used for solving the mesh file created by GAMBIT. The Pressure-based solver with implicit formulation was used for simulating the present module. Gradient evaluation was performed by Green-Gauss theorem. The k-ε realizable turbulent flow model was chosen for analyzing flow in the present module [24].Additionally, SIMPLEC (Simple-Consistent) scheme was applied because of high Reynolds number flow.

4 Results and discussion

4.1 Hydrodynamic Simulation

4.1.1. Velocity Field in the default interior

Fig. 2 (a-I), (a-II) depicts the velocity profiles in the default interior of the module under varying stirrer speed but at a fixed transmembrane pressure (TMP). Evidently, the stirrer rotation within the cylinder generates high-strength vortices in the default interior. The vortex strength necessarily increases with the increasing rotational speed, which helps to alleviate the CP and subsequent membrane fouling.

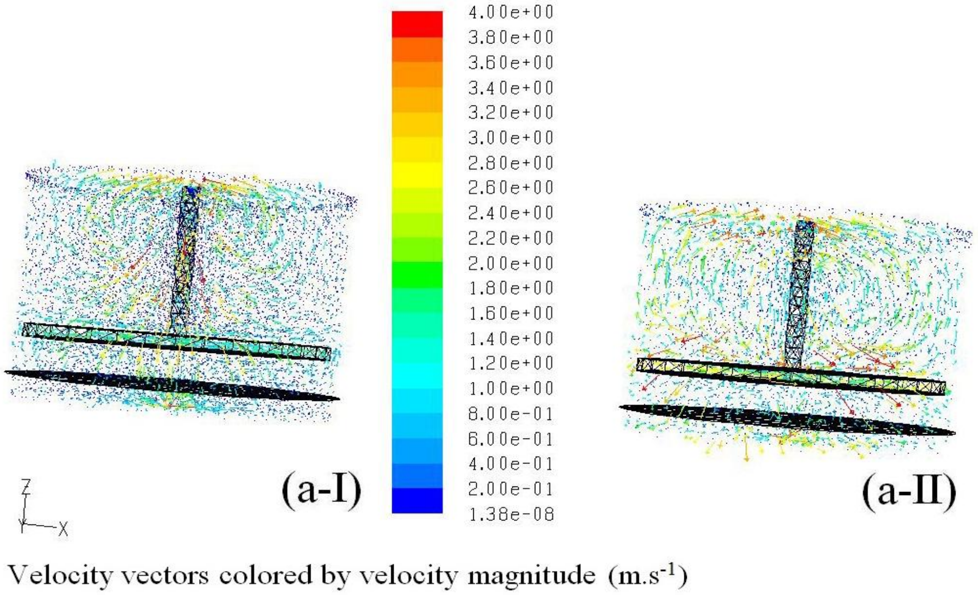

Fig. 2: Distribution of velocity vector in default interior of single stirred cell for TMP = 552 kPa (a-I) Ω = 47.1.rad $s^{-1}$and (a-II) Ω = 63.3 rad s^{-1}

4.1.2. Pathline variation

Fig.3 (a-I) and (a-II) displays the pathlines traced by the fluid particle, once again, under varying rotational speed but at a fixed TMP. The figure clearly justifies our claim of high-strength vortex flow at all stirrer speeds. Several vortices are noted to exist close to the membrane surface. Moreover, strong vortex flow is also suggested near the feed inlet. Overall, the vortices in the default interior are observed to cluster near the curved surface of the cylinder as well as near the base. The circulating pathlines over the membrane surface (i.e., the base) are expected to generate high back transport flux.

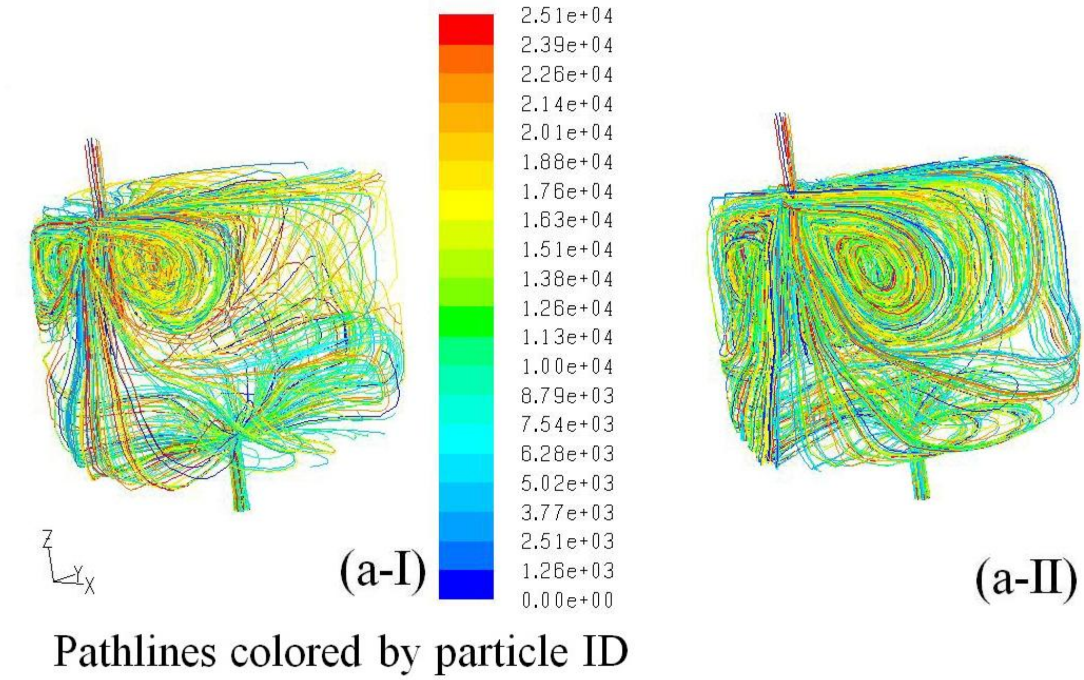

Fig. 3: Pathline in default interior of single stirred cell for TMP = 552 kPa (a-I)Ω = 47.1.rad s^{-1}and (a-II) Ω = 63.3 rad s^{-1}

4.1.3. Contour of Velocity magnitude

We have specifically focused on the velocity magnitude on the membrane surface before investigating the shear field and relevant turbulent properties like turbulent kinetic energy (k) and kinetic energy dissipation rates (ε). Fig.4 shows the variations of velocity magnitude at two different rotational speeds (i.e. Ω = 47.1 -rad s^{-1} and 63.3 rad s^{-1}). Naturally, the velocity magnitude was noted to increase with the stirrer speed. Consequently, we may expect high k and ε profiles at higher rotational speed.

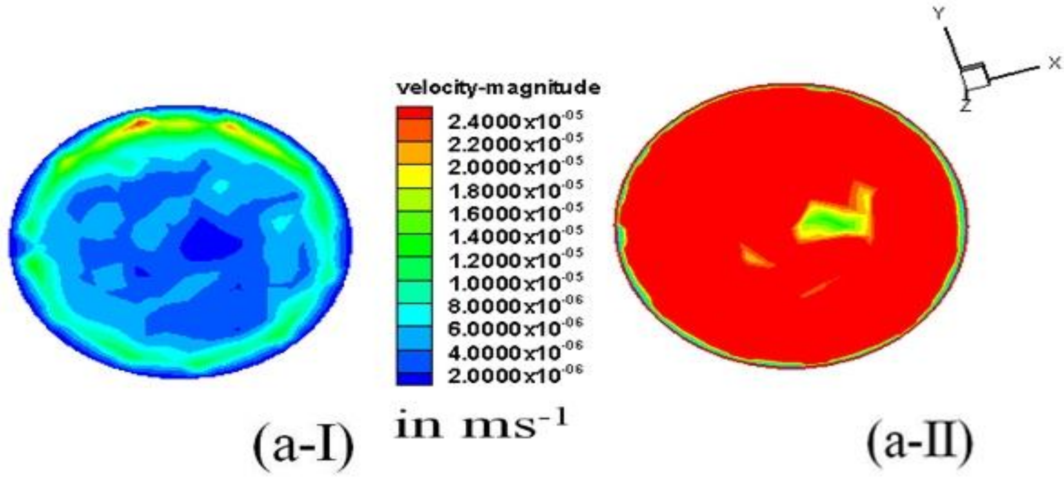

Fig. 4: Velocity magnitude on membrane surface of single stirred cell for TMP = 552 kPa (a-I) Ω = 47.1 rad s^{-1}and (a-II) Ω = 63.3 rad s^{-1}

4.1.4. Contour of Turbulent Kinetic Energy

Fig.5 shows the variation of turbulent kinetic energy on the stirrer as well as on the membrane with varying rotational speed but at a fixed TMP. It may be noted that the turbulent kinetic energy is the mean kinetic energy per unit mass associated with eddies in turbulent flows. The figure clearly indicates higher k value profiles at higher **Ω**. The k-profile has a direct connection with the solute scoop-up rate from the membrane surface. Thus, we may conclude an effective scoop-up action at higher stirrer speed.

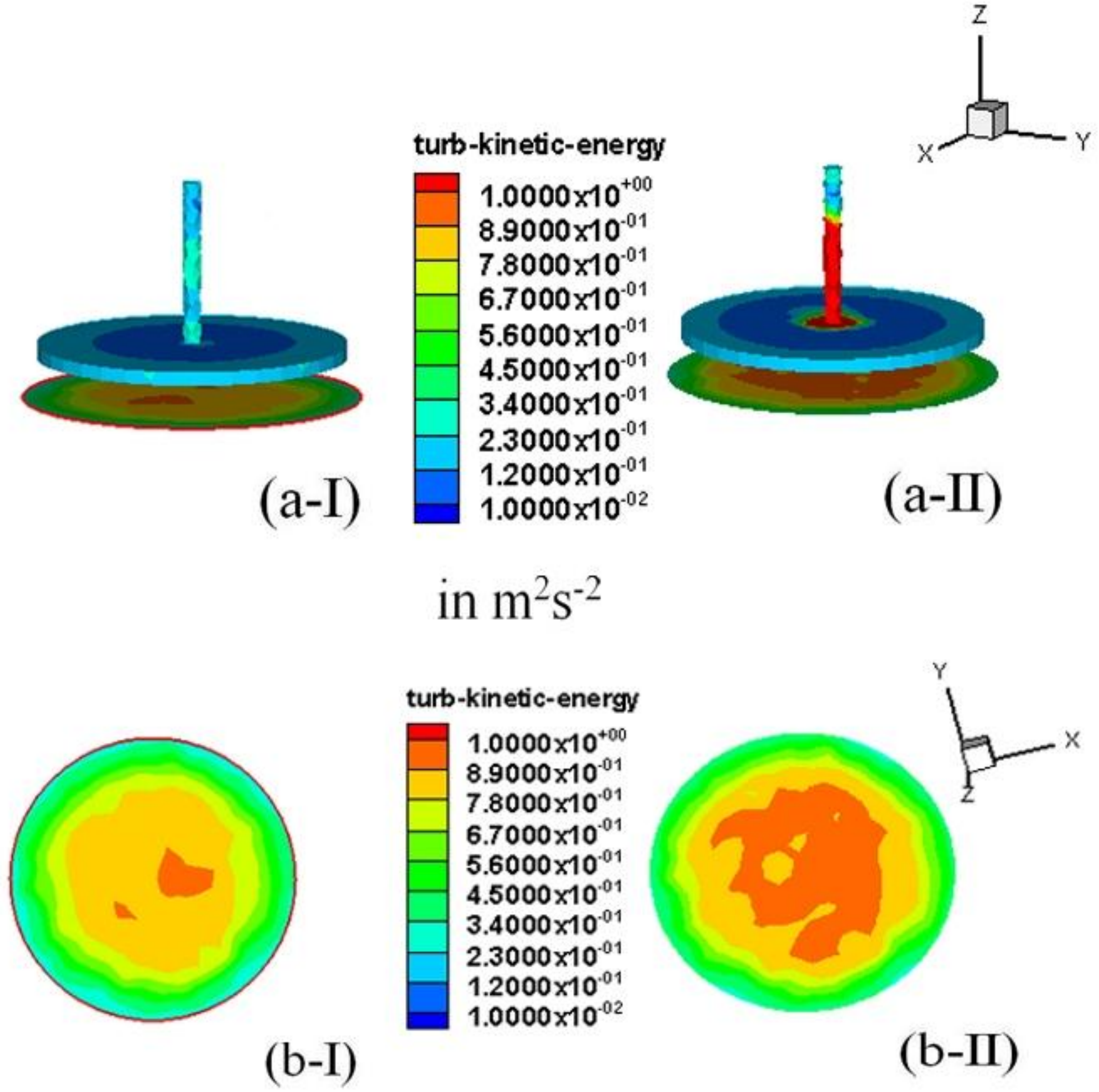

Fig. 5: Turbulent kinematic energy on rotating disk with shaft and membrane of single stirred cell at TMP = 552 kPa (a-I) Ω = 47.1 rad $s^{-1}$and (a-II) Ω = 63.3 rad $s^{-1}$and on membrane surface at TMP = 552 kPa (b-I) Ω = 47.1 rad $s^{-1}$and (b-II) Ω = 63.3 rad s^{-1}.

4.1.5. Contour of Turbulence Dissipation Energy

Fig. 6 displays the profiles of kinetic energy dissipation energy on the rotating disk as well as on the membrane surface. Similar to the other profiles, the variations of ε were simulated under two different rotational speeds. Turbulence dissipation represents the viscous conversion of the mechanical energy finally into heat. Higher rate of dissipation essentially signifies energy cascading to the scale of the smallest size eddies, which are in the order of molecular dimension. Therefore, high dissipation rate alternatively indicates a high energy release in the length scale of the deposited solute molecules (e.g., proteins and other macromolecule for ultrafiltration), which further specifies efficient energy cascading of the mechanical work done by the stirrer to the microscopic lift work on the deposited solute molecules. Naturally, the smooth energy cascade helps to dislodge the solutes from the membrane surface and helps to reduce the extent of CP.

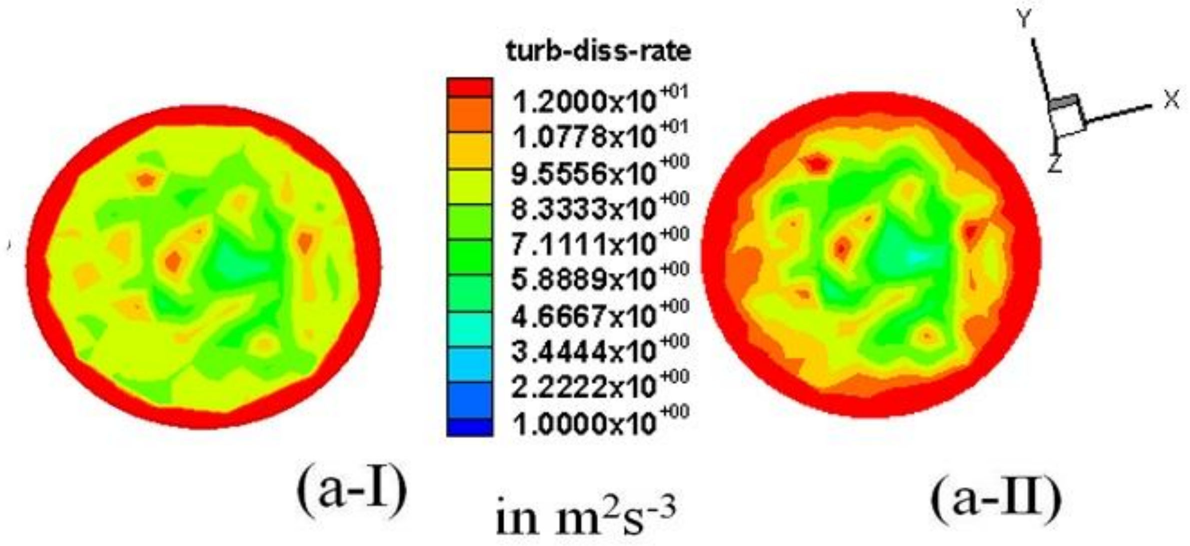

Fig. 6: Turbulence dissipation energy on membrane surface of single stirred cell for TMP = 552 kPa (a-I)Ω = 47.1rad $s^{-1}$and (a-II) Ω = 63.3 rad s^{-1}

5. Conclusion

Hydrodynamic simulation, using the standard CFD packages of GAMBIT and FLUENT, of a baseline Dynamic Shear Enhanced membrane module; namely, the single-stirred cell is performed in the present study. . The realizable k-ε turbulent model was used for this purpose. The results undeniably show the favorable effects of the stirrer speed on the profiles of velocity magnitude, vortex strength, turbulent kinetic energy, and kinetic energy dissipation rates. The said hydrodynamic variables followed an increasing trend with the stirrer speed over the entire default interior of the module. The hydrodynamic intensification helps to increase the scoop-up rate of the accumulated solutes from the membrane surface, which finally, is expected to result in reduced polarization effect and enhanced permeate throughput.

6. Nomenclature

TMP transmembrane pressure (kPa)

Greek letters

Ω rotational speed of the basket (rad s^{-1})

References

[1] K.K. Ng, C.F. Lin, S.C. Panchangam, P.K.A. Hong, P.Y. Yang, Reduced membrane fouling in a novel bio-entrapped membrane reactor for treatment of food and beverage processing wastewater, Wat. Res. 45 (14), 2011, 4269-4278.

[2] S. S. Sablani, M. F. A. Goosen, R. Al-Belushi, M. Wilf, Concentration polarization in ultrafiltration and reverse osmosis: a critical review, Desalination, 141, 2001, 269–289.

[3] M. Mulder, Basic Principles of Membrane Technology (Dordrecht, 2nd ed Kluwer Academic Publishers, 1996).

[4] A. Sarkar, S. Moulik, D. Sarkar, A. Roy, C. Bhattacharjee, Performance characterization and CFD analysis of a novel shear enhanced membrane module in ultrafiltration of Bovine Serum Albumin (BSA), Desalination, 292, 2012, 53–63.

[5] K. H. Youm, A.G Fane, D. E. Wiley, Effect of natural convection instability on membrane performance in dead end and cross flow ultrafiltration, J. Membrane Sci., 116, 1996, 229.

[6] S. S. L. Peppin, J. A. W. Elliott, Non-equilibrium thermodynamics of concentration polarization, Adv. Colloid Interface Sci. 92, 2001, 1.

[7] W. N. Gill, D. E. Wiley, C. J. D. Fell, A. G. Fane, Viscosity effect on concentration polarization, AlChE J. 34, 2004, 1563.

[8] D. R. Trettin, M. R. Doshi, Limiting flux in ultrafiltration of macromolecular solutions, Chem. Engg. Commun., 4, 1980, 507.

[9] T. R. Mollee, Y. G. Annisimov, M. S. Roberts, Periodic electric field enhanced transport through membrane, J. Membrane Sci. 278, 2006, 28.

[10] A. D. Enevoldsen, E. B. Hansen, G. Jonsson, Electro ultrafiltration of industrial enzyme solution, J. Membrane Sci. 299, 2007, 28.

[11] H. M. Wang, C. Y. Li, S. J. Chen, T. N. Cheng, T. L. Chan, Abatement of concentration polarization in ultrafiltration using n- hexadecane/water two-phase flow, J. Membrane Sci., 238, 2004, 1.

[12] Z. Cui, T. Taha, Enhancement of ultrafiltration using gas sparging: a comparison of different membrane module, J. Chem. Technol. Biotechnol., 78, 2003, 249.

[13] C. Bhattacharjee, S. Datta, Simulation of continuous stirred ultrafiltration process: an approach based on analytical solution couples with turbulent back transport, J. Chem. Technol. Biotechnol., 78, 2003, 1135-1141.

[14] C. Bhattacharjee, S. Datta, Analysis of mass transfer during ultrafiltration of PEG-6000 in a continuous stirred cell: effect of back transport, J. Membr. Sci., 119, 1996, 39-46.

[15] M. Y. Jaffrin, Dynamic shear-enhanced membrane filtration: a review of rotating disks, rotating membranes and vibrating systems., J. Membr. Sci., 324, 2008, 7-25.

[16] L. H. Ding, M. Y. Jaffrin, M. Mellal, G. He, Investigation of performances of a multishaft disk (MSD) system with overlapping membranes in microfiltration of mineral suspensions, J. of Membr. Sci., 276, 2006, 232-240.

[17] B. Halström, M. Lopez-Liva, Description of rotating ultrafiltration module, Desalination, 24, 1977, 39.

[18] M.Y. Jaffrin, G. He, L.H. Ding, P. Paullier, Effect of membrane overlapping on performance of multishaft rotating ceramic disk membranes, Desalination, 200, 2006, 269–271.

[19] R. Bouzerar, P. Paullier, M.Y. Jaffrin, Concentration of mineral suspensions and industrial effluent using a rotating disk dynamic filtration module, Desalination, 158, 2003, 79–85.

[20] C. Bhattacharjee, P.K. Bhattacharya, Ultrafiltration of black liquor using rotating disk membrane module, Sep. Purif. Technol., 49, 2006, 281–290.

[21] D. Sarkar, C. Bhattacharjee, Modeling and analytical simulation of rotating disk ultrafiltration module, J. Membr. Sci., 320, 2008, 344–355.

[22] D. Sarkar, D. Datta, D. Sen, C. Bhattacharjee, Simulation of continuous stirred rotating disk-membrane module: an approach based on surface renewal theory, Chem. Eng. Sci., 66, 2011, 2554–2567.

[23] J. S. Shen and R. F. Probstein, On the prediction of limiting flux in laminar ultrafiltration of macromolecular solution, Ind. Eng. Chem. Fundam., 16, 1977, 459.

[24] M. Naskar, K. Rana, D. Chatterjee, T. Dhara, R. Sultana, D. Sarkar, Design, performance characterization and hydrodynamic modeling of intermeshed spinning basket membrane (ISBM) module, Chemical Engineering Science, 206, 2019, 446–462.